Inorganic Chemistry

Article

pubs.acs.org/IC

Coordination versus Coupling of Dicyanamide in Molybdenum and Manganese Pyrazole Complexes

Marta Arroyo, Patricia Gómez-Iglesias, Jose Miguel Martín-Alvarez, Celedonio M. Alvarez, Daniel Miguel, and Fernando Villafañe*

IU CINQUIMA/Química Inorgánica, Facultad de Ciencias, Universidad de Valladolid, 47005 Valladolid, Spain

Supporting Information

ABSTRACT: The reactions of *cis*-[MoCl(η^3-methallyl)(CO)$_2$(NCMe)$_2$] (methallyl = CH$_2$C(CH$_3$)CH$_2$) with Na(NCNCN) and pz*H (pzH, pyrazole, or dmpzH, 3,5-dimethylpyrazole) lead to *cis*-[Mo(η^3-methallyl)(CO)$_2$(pz*H)-(μ-*N*CNC*N*-κ^2*N,N*)]$_2$ (pzH, **1a**; dmpzH, **1b**), where dicyanamide is coordinated as bridging ligand. Similar reactions with *fac*-[MnBr-(CO)$_3$(NCMe)$_2$] lead to the pyrazolylamidino complexes *fac*-[Mn(pz*H)-(CO)$_3$(*N*H═C(pz*)NC*N*-κ^2*N,N*)] (pzH, **2a**; dmpzH, **2b**), resulting from the coupling of pyrazol with one of the CN bonds of dicyanamide. The second CN bond of dicyanamide in **2a** undergoes a second coupling with pyrazole after addition of 1 equiv of *fac*-[MnBr(CO)$_3$(pzH)$_2$], yielding the dinuclear doubly coupled complex [{*fac*-Mn(pzH)(CO)$_3$}$_2$(μ-*N*H═C(pz)NC(pz)═*N*H-κ^4*N,N,N,N*)]Br (**3**). The crystal structure of **3** reveals the presence of two isomers, cis or trans, depending on whether the terminal pyrazoles are coordinated at the same or at different sides of the approximate plane defined by the bridging bis-amidine ligand. Only the cis isomer is detected in the crystal structure of the perchlorate salt of the same bimetallic cation (**4**), obtained by metathesis with AgClO$_4$. All the N-bound hydrogen atoms of the cations in **3** or **4** are involved in hydrogen bonds. Some of the C−N bonds of the pyrazolylamidino ligand have a character intermediate between single and double, and theoretical studies were carried out on **2a** and **3** to confirm its electronic origin and discard packing effects. Calculations also show the essential role of bromide in the planarity of the tetradentate ligand in the bimetallic complex **3**.

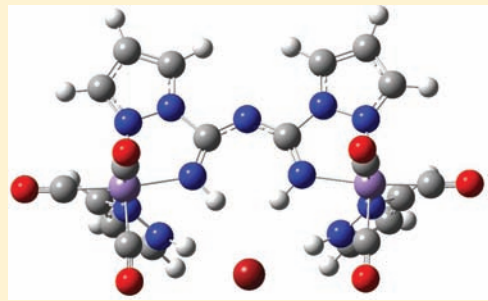

■ INTRODUCTION

We have recently described new pyrazolylamidino complexes obtained from the reactions of pyrazoles and nitriles in the presence of manganese- and rhenium(I) metal centers.[1] There are not many examples of this reaction,[1,2] even though pyrazolylamidino ligands present several interesting features: (a) they are synthesized in situ by an addition of the N−H bond of the pyrazole across the nitrile C−N triple bond (Scheme 1);[3] thus, using different nitriles and pyrazoles may give rise to new bidentate chelating ligands of distinct electronic and steric properties; (b) the NH group may give rise to further reactivity, as it may be involved in noncovalent interactions or may be deprotonated; (c) the different properties of the two donor atoms and the electron delocalization within the ligand makes them potentially interesting for electron transfer processes and related physical properties. The mechanism of this reaction remains unclear, although it is generally assumed to be a intramolecular nucleophilic attack of the pyrazole to the nitrile,[2f,k] intermolecular paths have been also proposed, depending on the electronic configuration of the metal center.[2b]

Scheme 1. General Method for the Synthesis of Pyrazolylamidino Complexes

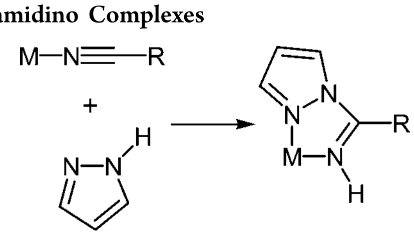

Considering the possibility of using different precursors, we decided to extend this study to sodium dicyanamide, which contains two CN bonds capable of undergoing nucleophilic addition by pyrazoles. In fact, the coupling of pyrazoles and pseudohalides such as dicyanamide, tricyanomethanide, or nitrosodicyanomethanide to form new chelating ligands have already been described for different transition metals.[4] In our case, the behavior of the dicyanamide/pyrazole system depends on the metallic substrate used.

■ RESULTS AND DISCUSSION

Molybdenum Complexes. The reactions of *cis*-[MoCl(η^3-methallyl)(CO)$_2$(NCMe)$_2$] with Na(NCNCN) and pzH or dmpzH in a 1/1/1 ratio in tetrahydrofuran (thf) at 60 °C for 1 h lead to *cis*-[Mo(η^3-methallyl)(CO)$_2$(pzH)(μ-*N*CNC*N*-κ^2*N,N*)]$_2$ (**1a**), or *cis*-[Mo(η^3-methallyl)(CO)$_2$(dmpzH)(μ-*N*CNC*N*-κ^2*N,N*)]$_2$ (**1b**), as yellow solids (Scheme 2). The

Received: December 6, 2011
Published: May 15, 2012

dx.doi.org/10.1021/ic202631c | Inorg. Chem. 2012, 51, 6070−6080

Scheme 2. Syntheses of Complex 1

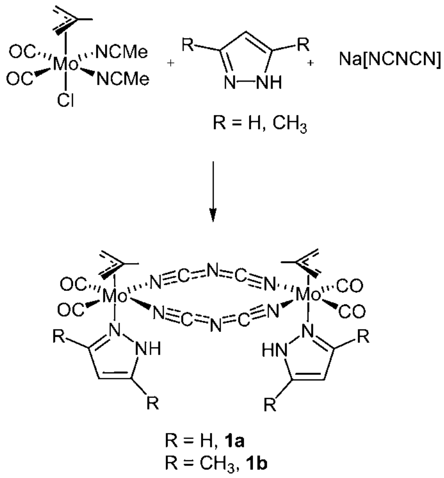

same products are obtained when excess of pyrazole is used. Pyrazolylamidino complexes were never detected even when more drastic reaction conditions were used. This can not be considered surprising, since no pyrazolylamidino products could be isolated when *cis*-[MoCl(η^3-methallyl)-$(CO)_2(NCMe)_2$] was treated with pyrazoles in acetonitrile. These results contrast with the report of the only pyrazolylamidino molybdenum complex reported so far, *fac*-[MoBr(η^3-allyl)$(CO)_2$(*N*H=C(CH_3)pz-κ^2*N,N*)], described in 1987 after the reaction of *fac*-[Mo$(CO)_3(NCMe)_3$] with Na[Me_2Ga(pz)$(OC_6H_4NH_2)$] and allylbromide.[2j]

Compound **1b** could be crystallografically characterized (Figure 1 and Table 1).[5] The resulting determination is poor

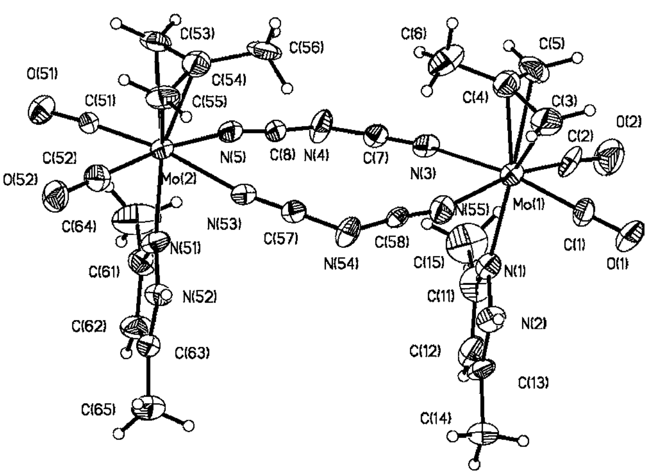

Figure 1. Perspective view of *cis*-[Mo(η^3-methallyl)$(CO)_2$(dmpzH)-(μ-*N*CNC*N*-κ^2*N,N*)$]_2$ (**1b**), showing the atom numbering. Ellipsoids are drawn at 30% probability.

(high residuals) because of the low quality of the crystal, but the structure is included here since it confirms unambiguously the connectivity of the molecule. Both molybdenum atoms are pseudo-octahedrally coordinated, assuming that the methallyl group occupies one site. The terminal carbon atoms of the methallyl group are oriented over the carbonyl groups, as has been demonstrated to be the most energetically favorable arrangement.[6] The complex is a quasi-symmetric dimer where two dicyanamides bridge two "*cis*-Mo(η^3-methallyl)-$(CO)_2$(dmpzH)" fragments, with the methallyl and dimethylpyrazole coordinated respectively trans. Only one of the two possible diastereomers is detected in the structure: that with both methallyl (or both pyrazoles) at the same side of the approximate plane formed by the bridging dicyanamides and the metal centers. A wide range of bimetallic complexes with bridging dicyanamide are known,[7] although we have not been able to find any precedent containing molybdenum.

Table 1. Selected Distances (Å) and Angles (deg.) for *cis*-[Mo(η^3-methallyl)$(CO)_2$(dmpzH)(μ-*N*CNC*N*-κ^2*N,N*)$]_2$ (1b)[5]

Mo(1)−C(1)	2.03(3)
Mo(1)−C(2)	1.99(3)
Mo(1)−N(1)	2.29(2)
Mo(1)−N(3)	2.19(2)
Mo(1)−N(55)	2.34(2)
C(1)−Mo(1)−C(2)	79.7(11)
C(1)−Mo(1)−N(3)	169.6(9)
C(2)−Mo(1)−N(3)	99.3(9)
C(1)−Mo(1)−N(1)	86.1(9)
C(2)−Mo(1)−N(1)	86.8(10)
N(3)−Mo(1)−N(1)	83.5(8)
C(1)−Mo(1)−N(55)	98.1(10)
C(2)−Mo(1)−N(55)	166.3(10)
N(1)−Mo(1)−N(55)	79.6(7)
N(3)−Mo(1)−N(55)	80.3(7)

The NMR spectra of **1a** and **1b** are not informative (see Experimental Section). Both are very scarcely soluble, and their spectra in Me_2CO-*d*[6] or thf-*d*[8] display mixtures which can not be identified. In an attempt to brake these processes in solution, the NMR spectra were recorded immediately after dissolving the solids at low temperature, but mixtures of the complexes were also obtained. There are several reasons to explain the origin of the species detected in the NMR spectra. The isomer found in the solid structure may be described as cis, but the presence of a trans isomer in solution can not be discarded. On the other hand, allyldicarbonylmolybdenum(II) complexes usually display a nondissociative trigonal twist process in which there is an intramolecular rotation of the XL_2 triangular face,[8] which would afford new sets of signals if it were slow enough. Finally, the well-known lability of the metal-nitrile bonds (Mo-NCNCN bonds in **1a** and **1b**), would lead to decoordination of dicyanamide and eventually to the decomposition of the complex, and in fact the solutions became brown in a few minutes.

The IR spectra of **1a** and **1b** show two bands in the C−O stretching region in solution, as expected for their *cis*-dicarbonyl geometry. The frequencies are slightly higher for the complex with pzH than those with dmpzH, as could be predicted considering the better donor properties of dmpzH compared to pzH.

Manganese Mononuclear Complexes. The reactions of *fac*-[MnBr$(CO)_3(NCMe)_2$] with Na(NCNCN) and pzH or dmpzH in a 1/1/2 ratio in thf at 60 °C for 6 h lead to *fac*-[Mn(pzH)$(CO)_3$(*N*H=C(pz)NCN-κ^2*N,N*)] (**2a**), or *fac*-[Mn(dmpzH)$(CO)_3$(*N*H=C(dmpz)NCN-κ^2*N,N*)] (**2b**), as yellow solids (Scheme 3, path "a"). The same products, although in lower yields, are obtained when 1 equiv of the pyrazole is used.

The IR spectra of **2a** and **2b** show three bands in the C−O stretching region in solution, as expected for their *fac*-tricarbonyl geometry. As described above for the molybdenum

Scheme 3. Syntheses of Complexes 2 and 3

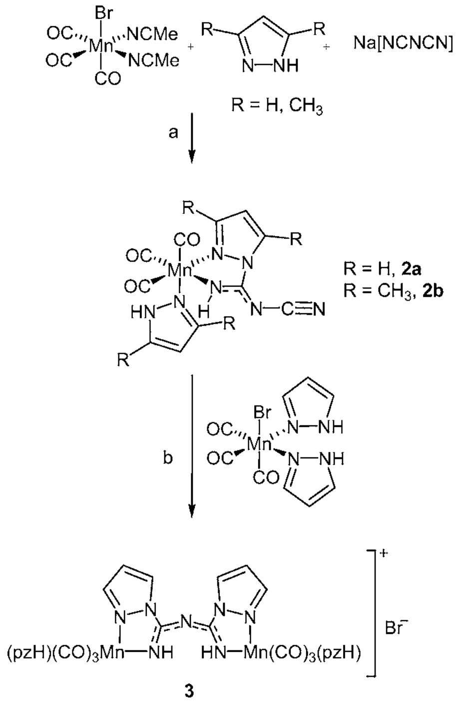

complexes, the frequencies are slightly higher for the complex with pzH than those with dmpzH, as could be predicted considering the better donor properties of dmpzH compared to pzH.

The NMR data (see Experimental Section) of the new complexes do not provide important structural information, except for a previously observed feature in complexes containing both pyrazole and pirazolylamidino ligands, which is the higher chemical shifts of the latter compared to coordinated pyrazoles,[1c] or to the values previously reported for coordinated nitrile.[9] The characterization in solution of **2b** was difficult because of its low stability and low solubility in solution. The low stability generated ^{1}H NMR spectra always containing more signals than those expected, because of the formation of different byproducts which could not be identified (vide infra). Both complexes, **2a** and **2b**, could be crystallographically characterized (Figure 2 and Table 2).

Both structures confirm the coordination of a pyrazolylamidino ligand resulting from the addition of the N−H bond of the pyrazole across one of the CN triple bonds in dicyanamide. As far as we know, these are the first pyrazolylamidino complexes crystallographically characterized that are derived from the coupling of dicyanamide.

The structural data are essentially the same in both complexes, and very similar to those found in previously reported structures of halotricarbonylmanganese(I) complexes containing a bidentate N-donor ligand.[10] The distances and angles found in the pyrazolylamidino ligands are also similar to those found in pyrazolylamidino complexes obtained from monodentate nitriles.[1,2]

The N-bound hydrogens are involved in intramolecular hydrogen bonds with the free nitrogen atom in the dicyanamide of an adjacent molecule [H(3)···N(7) 2.75 Å and H(5)···N(7) 1.99 Å for **2a**; H(3)···N(7) 2.46 Å and H(5)···N(7) 2.08 Å for **2b**]. These and the corresponding N···N distances (3.313 and 2.845 Å for **2a**, and 3.146 and 2.936 Å for **2b**, respectively) and

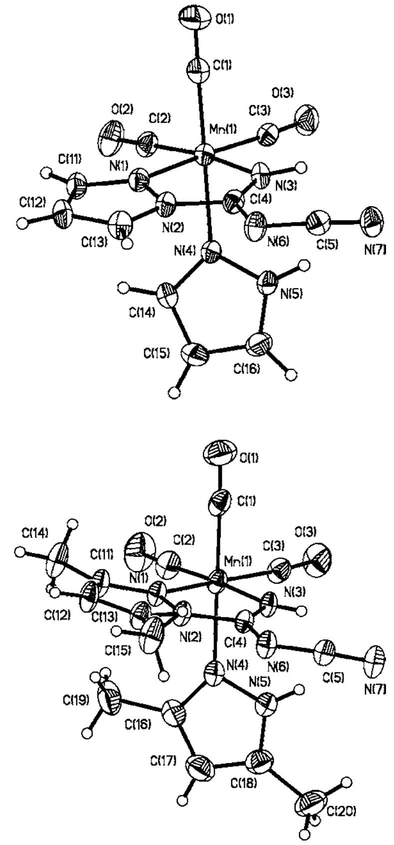

Figure 2. Perspective view of *fac*-[Mn(pzH)(CO)$_3$(*N*H=C(pz)-NCN-κ^2*N,N*)] (**2a**) (above), and *fac*-[Mn(dmpzH)(CO)$_3$(*N*H=C(dmpz)NCN-κ^2*N,N*)] (**2b**) (below), showing the atom numbering. Ellipsoids are drawn at 30% probability.

N−H···N angles (125 and 178° for **2a**, and 137 and 174° for **2b**, respectively) confirm the presence of a hydrogen bond which may be considered between "weak" and "moderate".[11]

Two resonance forms may be drawn for the new pyrazolylamidino ligand derived from dicyanamide, depending on which nitrogen atom is bearing the negative charge (Scheme 4). In resonance form A, the negative charge is located on the nitrogen donor atom; therefore, it is the expected for a traditional anionic ligand. In form B, the negative charge is placed on the central nitrogen atom of dicyanamide, thus giving rise to a zwitterionic complex. The N(3)−C(4) and C(4)−N(6) distances in the crystal structures (Table 2) are very similar [1.286(4) vs 1.332(4) for **2a**, and 1.296(4) vs 1.342(4) for **2b**] and seem to point to a resonance hybrid where both resonance forms contribute similarly. However, the similarity of that bond distances may have been caused either by electronic or by packing effects, and therefore a theoretical study was carried out on **2a** to determine the origin of that feature. Starting from the crystallographic coordinates, the geometry was optimized using density functional theory (DFT) methods (see Experimental Section) reaching a minimum with bond distances and angles that compare well with the experimental ones (Figure 3 and Table 2). A NBO study was then performed on the minimum geometry to calculate the Wiberg indexes of the two N−C bonds, and the results are collected in Table 2. The Wiberg indexes of the N(3)−C(4) and C(4)−N(6) bonds are 1.40 and 1.42, respectively, indicating that both bonds have a bond order intermediate between single and double. Therefore, the similarity in the values of those bond distances

Table 2. Selected Distances (Å) and Angles (deg.) for *fac*-[Mn(pzH)$(CO)_3$(*N*H=C(pz)NCN-κ^2*N,N*)] (2a), and *fac*-[Mn(dmpzH)$(CO)_3$(*N*H=C(dmpz)NCN-κ^2*N,N*)] (2b), DFT-Optimized Distances (Å) and Angles (deg.) for 2a and Wiberg Bond Indexes for Selected Distances

	2a	2b	2a (calcd)	Wiberg index
Mn(1)–C(1)	1.795(4)	1.815(5)	1.817	0.91
Mn(1)–C(2)	1.803(4)	1.816(4)	1.811	0.93
Mn(1)–C(3)	1.798(4)	1.822(4)	1.819	0.90
Mn(1)–N(1)	2.026(2)	2.063(3)	2.066	
Mn(1)–N(3)	2.041(2)	2.028(3)	2.069	
Mn(1)–N(4)	2.070(2)	2.115(3)	2.124	
C(4)–N(3)	1.286(4)	1.296(4)	1.328	1.40
C(4)–N(6)	1.332(4)	1.342(4)	1.316	1.42
N(2)–C(4)	1.419(4)	1.426(4)	1.422	0.95
C(1)–Mn(1)–C(3)	88.41(14)	88.50(17)	92.04	
C(1)–Mn(1)–C(2)	90.06(15)	88.8(2)	92.34	
C(3)–Mn(1)–C(2)	89.61(13)	87.77(17)	93.28	
C(1)–Mn(1)–N(3)	94.24(13)	94.04(16)	90.19	
C(3)–Mn(1)–N(3)	97.50(12)	94.92(14)	94.77	
C(2)–Mn(1)–N(3)	171.78(12)	176.12(16)	171.47	
C(1)–Mn(1)–N(1)	92.89(13)	89.88(15)	91.40	
C(3)–Mn(1)–N(1)	175.00(11)	171.38(14)	171.15	
C(2)–Mn(1)–N(1)	95.21(11)	100.67(14)	94.72	
N(3)–Mn(1)–N(1)	77.60(9)	76.75(11)	77.07	
C(1)–Mn(1)–N(4)	178.76(13)	179.06(15)	176.66	
C(3)–Mn(1)–N(4)	92.63(12)	92.16(15)	89.28	
C(2)–Mn(1)–N(4)	90.62(11)	91.87(17)	90.65	
N(3)–Mn(1)–N(4)	84.96(9)	85.24(13)	86.64	
N(1)–Mn(1)–N(4)	86.01(9)	89.37(12)	86.86	

Scheme 4. Resonance Forms Proposed for the New Pyrazolylamidino Ligand Derived from Dicyanamide

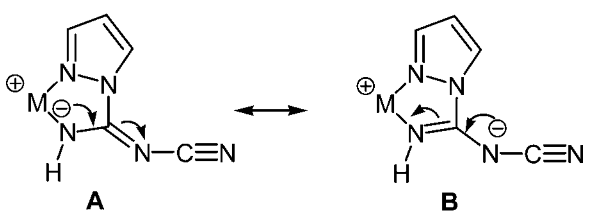

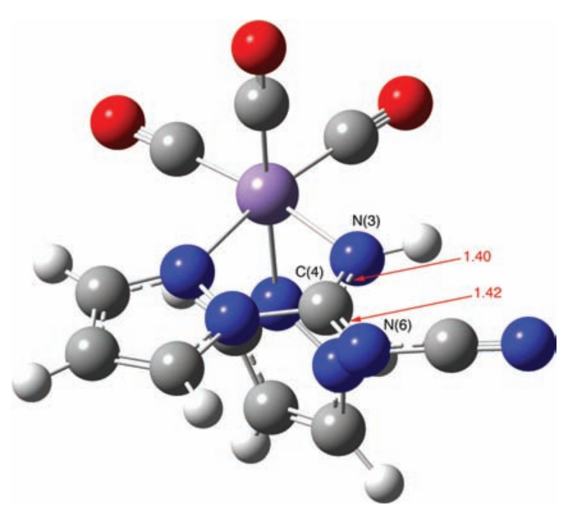

Figure 3. Wiberg indexes of the relevant C–N bonds obtained from the theoretical study on **2a**.

has an electronic origin and is not due to packing effects. It may be concluded, then, that the best description for this ligand is that depicted in Scheme 3 where the bond order from both N–C bonds derived from dicyanamide is 1.5.

Manganese Binuclear Complexes. When **2a** is maintained in solution in the reaction mixture, a new bimetallic complex [{*fac*-Mn(pzH)$(CO)_3$}$_2$(μ-*N*H=C(pz)NC(pz)=*N*H-κ^4*N,N,N,N*)]Br, **3**, is obtained as a mixture of isomers. The formation of this complex may be interpreted considering the process depicted in Scheme 3 (path "b"). The uncoordinated C≡N present in **2a** may undergo a coupling process with a second pyrazol. This second pyrazol should come from the bis(pyrazol) complex, *fac*-[MnBr$(CO)_3$$(pzH)_2$], which occurs as sideproduct in the coupling reactions to obtain pyrazolylamidino complexes.[1] Therefore, the presence in solution of both **2a** and *fac*-[MnBr$(CO)_3$$(pzH)_2$] should give rise to a second coupling process, affording **3**. As indicated above, the mechanism of the coupling reaction is not straighforward, but it is evident that both pyrazole and coordinated nitrile must be in solution to obtain a pyrazolylamidino ligand.

The selective synthesis of **3** as a yellow solid was achieved from the reaction of **2a** with the stoichiometric amount of *fac*-[MnBr$(CO)_3$$(pzH)_2$] in thf at room temperature for 4 h. The attempts to isolate a similar complex to **3** with dmpzH, starting from **2b**, failed. As indicated before, **2b** is unstable in solution, and its ^{1}H NMR spectra show always minor unidentified signals, which could be due to a complex similar to **3**, but containing dmzH instead of pzH. However, all the attempts to isolate or to synthesize this compound selectively failed.

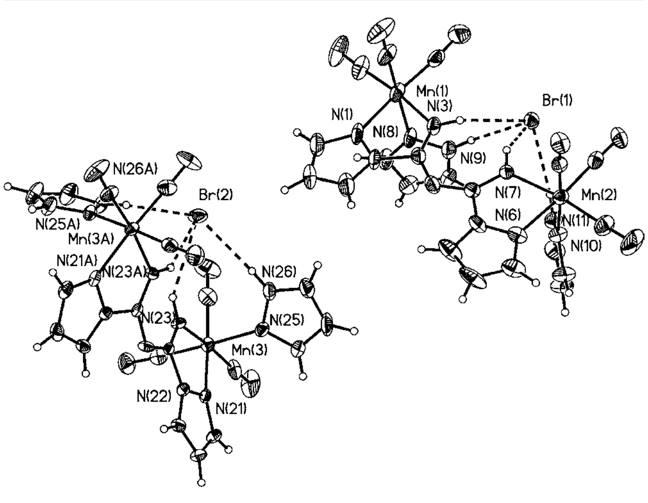

Figure 4. Perspective view of [{*fac*-Mn(pzH)$(CO)_3$}$_2$(μ-*N*H=C(pz)NC(pz)=*N*H-κ^4*N,N,N,N*)]Br (**3**) showing the atom numbering. Ellipsoids are drawn at 30% probability.

The crystal structure of **3** (Figure 4 and Table 3) reveals the presence of two isomers, depending on whether both coordinated pyrazols are situated at the same side (cis, right in Figure 4) or at opposite sides (trans, left in Figure 4) of the approximate plane defined by the bridging ligand and the metals. The complex is a dimer constituted by two "*fac*-Mn$(CO)_3$(pzH)" fragments linked by the new bis(pirazolylamidino) ligand "*N*H=C(pz)NC(pz)=*N*H-κ^4*N,N,N,N*", which bridges both metallic fragments. The new pyrazolylamidino ligand comes from the nucleophilic addition of one pyrazole to each C≡N group of dicyanamide, giving rise

Table 3. Selected Distances (Å) and Angles (deg) for [{*fac*-Mn(pzH)$(CO)_3$}$_2$(μ-*NH*=C(pz)NC(pz)=*NH*-κ^4*N,N,N,N*)]A (A = Br, 3; ClO_4, 4)[a]

	3 *cis* a	3 *cis* b	3 *trans*	4 *cis* a	4 *cis* b	*cis* calcd	*trans* calcd
Mn(1)−C(1)	1.791(13)	1.780(12)	1.786(11)	1.77(2)	1.85(2)	1.816	1.815
Mn(1)−C(2)	1.779(14)	1.811(12)	1.820(12)	1.73(2)	1.86(2)	1.831	1.833
Mn(1)−C(3)	1.814(12)	1.817(12)	1.800(11)	1.70(2)	1.88(3)	1.812	1.812
Mn(1)−N(1)	2.022(10)	2.015(8)	2.048(7)	2.005(18)	2.022(16)	2.054	2.057
Mn(1)−N(3)	2.021(7)	2.042(7)	2.029(6)	2.017(18)	2.054(17)	2.053	2.061
Mn(1)−N(8)	2.077(8)	2.091(8)	2.041(7)	2.068(19)	2.062(16)	2.121	2.115
N(1)−N(2)	1.344(12)	1.360(11)	1.357(9)	1.42(2)	1.31(2)	1.356	1.355
N(2)−C(14)	1.438(12)	1.406(11)	1.412(10)	1.37(2)	1.49(3)	1.436	1.432
N(3)−C(14)	1.291(12)	1.288(11)	1.283(10)	1.28(2)	1.33(2)	1.300	1.301
N(4)−C(14)	1.336(13)	1.327(11)	1.328(9)	1.30(2)	1.33(2)	1.337	1.335
C(1)−O(1)	1.151(13)	1.153(11)	1.141(11)	1.17(3)	1.12(3)	1.153	1.153
C(2)−O(2)	1.157(13)	1.132(12)	1.141(12)	1.20(3)	1.09(2)	1.150	1.150
C(3)−O(3)	1.136(13)	1.131(12)	1.124(11)	1.19(3)	1.11(3)	1.156	1.156
C(1)−Mn(1)−N(8)	177.5(4)	176.4(4)	176.6(3)	176.7(9)	177.4(9)	176.7	176.4
C(2)−Mn(1)−N(1)	174.8(4)	174.9(4)	175.0(3)	176.6(9)	173.3(9)	172.9	173.9
C(3)−Mn(1)−N(3)	173.4(5)	172.0(5)	173.1(4)	169.9(8)	173.9(9)	171.1	170.9
C(15)−N(4)−C(14)	123.7(8)		120.6(9)	123.3(9)		125.7	125.4

[a]The cis isomer does not have a crystallographic symmetry plane and, therefore, the two moieties of the molecule are not equivalent. Here we refer to one of the moieties as "*cis* a" and to the other moiety as "*cis* b".

a new tetradentate ligand. It is almost planar, as the dihedral angle formed by its two pirazolylamidino moieties differs 4° from planarity in the cis diastereomer and −16° in the trans diastereomer. As indicated by the different signs, the pirazolylamidino fragments are bent toward the same side in the cis isomer, but to opposite sides in the trans isomer.

A very interesting feature in the structure is the involvement of all the hydrogens bonded to nitrogen atoms in hydrogen bonds with the bromide. The N···H and N···Br distances are collected in Table 4, and confirm the presence of hydrogen bonds which may be considered as "weak".[11] To know the role of the anion in the structure, we decided to substitute the bromide by another anion able to form hydrogen bonds, such as perchlorate. Thus, the reaction of **3** with a stoichiometric amount of $AgClO_4$ in thf at room temperature, leads to [{*fac*-Mn(pzH)$(CO)_3$}$_2$(μ-*NH*=C(pz)NC(pz)=*NH*-κ^4*N,N,N,N*)]-ClO_4, **4**.

Table 4. Distances (Å) and Angles (deg.) for the Hydrogen Bonds with Bromide Ion Detected in the Crystal Structure of [{*fac*-Mn(pzH)$(CO)_3$}$_2$(μ-*NH*=C(pz)NC(pz)=*NH*-κ^4*N,N,N,N*)]Br (3)

N−H···Br	H···Br (Å)	N···Br (Å)	N−H···Br (deg.)
N(3)−H(3)···Br(1)	2.606	3.513	147
N(7)−H(7)···Br(1)	2.329	3.353	173
N(9)−H(9)···Br(2)	2.513	3.373	141
N(12)−H(12)···Br(2)	2.311	3.334	172
N(15)−H(15)···Br(2)	2.558	3.417	141
N(17)−H(17)···Br(2)	2.265	3.286	171

The crystal structure of **4** is shown in Figure 5, and selected distances and angles are collected in Table 3.[12] Only the cis diastereomer is detected in the crystal, since the pyrazoles are coordinated at the same side of the approximate plane defined by the bridging ligand and the metals. In this case, the tetradentate ligand is almost planar, since the dihedral angle defined by both pirazolylamidino moieties differs 2° from planarity, being bent toward the same side, as occurred for the cis isomer in **3**.

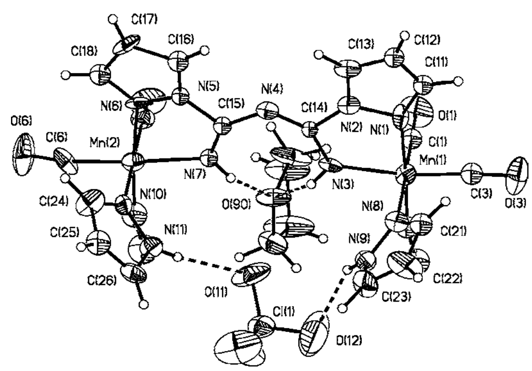

Figure 5. Perspective view of [{*fac*-Mn(pzH)$(CO)_3$}$_2$(μ-*NH*=C(pz)NC(pz)=*NH*-κ^4*N,N,N,N*)]ClO_4 (**4**) showing the atom numbering. Ellipsoids are drawn at 30% probability.

As expected, the perchlorate is involved in hydrogen bonds, but only with the hydrogens of the coordinated pyrazols [H(11)···O(11) 1.930 Å; and H(9)···O(12) 1.970 Å, with 2.930 Å for N(11)···O(11), and 2.831 Å for N(9)···O(12), being 163 and 139° the N−H···O angles]. These distances corrrespond to "moderate" hydrogen bonds,[11] as well as those where the hydrogen atoms of the bis(pyrazolylamidino) ligand derived from dicyanamide are involved, in this case with the oxygen atom of a thf molecule: H(3)···O(90) 2.159 and H(7)···O(90) 2.025 Å; with 3.060 for N(3)···O(90), and 2.928 Å for N(7)···O(90), with a value of 145° for both N−H···O angles.

As for the bidentate ligand derived from the coupling of pyrazole and one C≡N bond in dicyanamide present in complexes **2**, several resonance forms may be drawn for the new bis(pyrazolylamidino) tetradentate ligand present in complexes **3** and **4**, depending on which nitrogen atom is bearing the negative charge (Scheme 5). As before, the N(3)−C(14) and C(14)−N(4) distances in the crystal structures (Table 3) are very similar but, in this case, the structure

Scheme 5. Resonance Forms Proposed for the New Tetradentate Bis(pyrazolylamidino) Ligand Derived from Dicyanamide

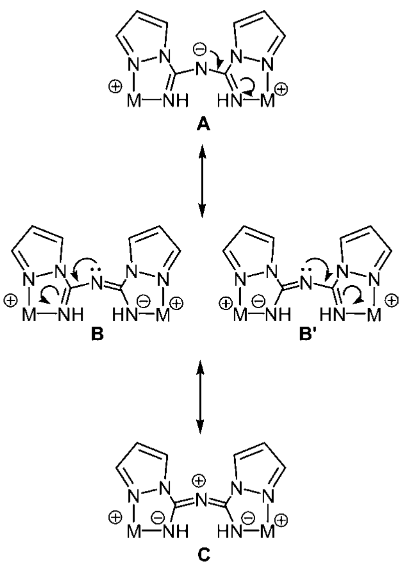

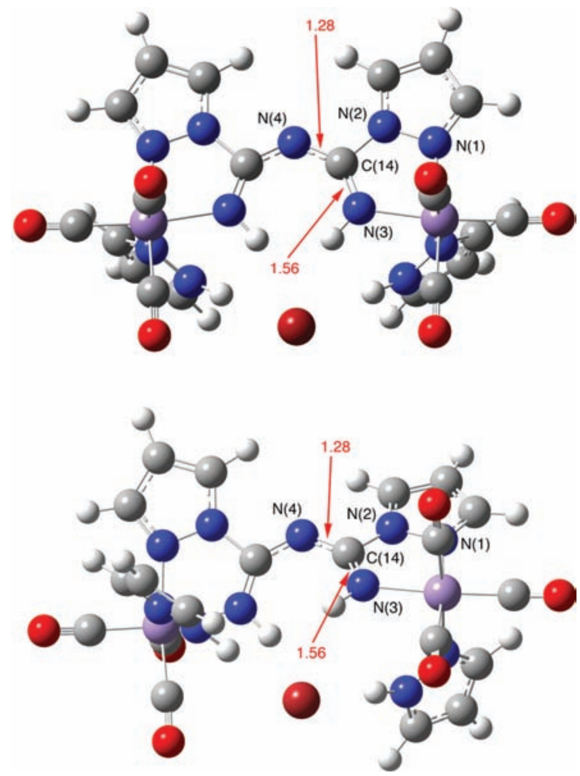

Figure 6. Wiberg bond indexes obtained from the theoretical study of [{*fac*-Mn(pzH)(CO)$_3$}$_2$(μ-*N*H═C(pz)NC(pz)═*N*H-κ^4*N,N,N,N*)]Br (**3**), cis isomer above and trans isomer below.

determination of **4** is not accurate enough to deduce the predominant resonance form. Thus, a new calculation was set and the same procedure followed for the study of **2a** was used to get the Wiberg indexes on the dinuclear complex **3** (for both trans and cis isomers). The results of this study are summarized in Table 5 and Figure 6, which displays the minimized structure

Table 5. Wiberg Bond Indexes of Selected Bonds of cis and trans Isomers of [{*fac*-Mn(pzH)(CO)$_3$}$_2$(μ-*N*H═C(pz)NC(pz)═*N*H-κ^4*N,N,N,N*)]Br (3)

	3 cis		3 trans	
	calcd bond dist.	Wiberg index	calcd bond dist.	Wiberg index
N(1)−N(2)	1.356	1.16	1.355	1.15
N(2)−C(14)	1.436	0.94	1.432	0.94
N(3)−C(14)	1.300	1.56	1.301	1.56
N(4)−C(14)	1.337	1.28	1.335	1.28

and the representative Wiberg indexes. The calculated bond distances compare well with the experimental ones and, as with the study carried out on **2a**, the packing effects can be ruled out as the cause of the C−N bond distances being intermediate between single and double bonds. The calculated Wiberg indexes of the N(3)−C(14) and C(14)−N(4) bonds are 1.56 and 1.28 respectively, in agreement with their intermediate character.

A curious feature arising from the theoretical study is that minimization of the bimetallic cis cation alone leads to a structure with the tetradentate bridging ligand twisted, being the dihedral angle defined by both pyrazolylamidino moieties of 38°. The planar structure found in the crystal structure corresponds to a transition state between the two twisted ground structures, as represented in Figure 7, with a calculated activation energy ΔE = 3.44 kcal/mol. Interestingly, the planar structure corresponding to a minimum of energy is only attained when the bromide anion is included in the calculation (Figure 8). Therefore, all the Wiberg index calculations have been performed on this ionic pair instead of on the isolated cation.

The NMR data for **3** is rather complicated because of the presence in solution of cis and trans isomers, therefore it will be discussed below, after discussing the NMR spectra of **4**, which is simpler since only the cis isomer is present in solution. Table 6 collects ^{1}H NMR data for **4** at different temperatures, Scheme 6 displays which protons are involved in the NOEs detected at 183 K, and Figure 9 collects the ^{1}H NMR spectra between 50 and −90 °C. The data collected in Table 6 clearly show that the pyrazoles are slightly unequivalent in all the range of temperatures registered (except for H^4pzH at room temperature (r.t.) and above, probably because of accidental degeneration), whereas the protons of both fragments in the bis(pyrazolylamidino) ligand are only unequivalent at low temperature, except for H^5pz, which are equivalent in all the range of temperatures registered. The latter feature may be explained considering an equilibrium between enantiomers similar to those detected in the calculations where the tetradentate bis(pyrazolylamidino) ligand is folded. The low energy of the enantiomers exchange indicates that the average situation, corresponding to a planar tetradentate bis(pyrazolylamidino) ligand, must be easily achieved (Figure 7, above). This would explain why the protons in the inner part of the ligand, that is, *H*NMn and H^3pz, are those more affected by the process, whereas that external such as H^5pz remains unaffected at different temperatures.

On the other hand, the presence of only the cis isomer in **4** is somewhat surprising, as **3** was a mixture of trans and cis. So far we have been unable to find a definitive explanation for this fact.

dx.doi.org/10.1021/ic202631c | Inorg. Chem. 2012, 51, 6070−6080

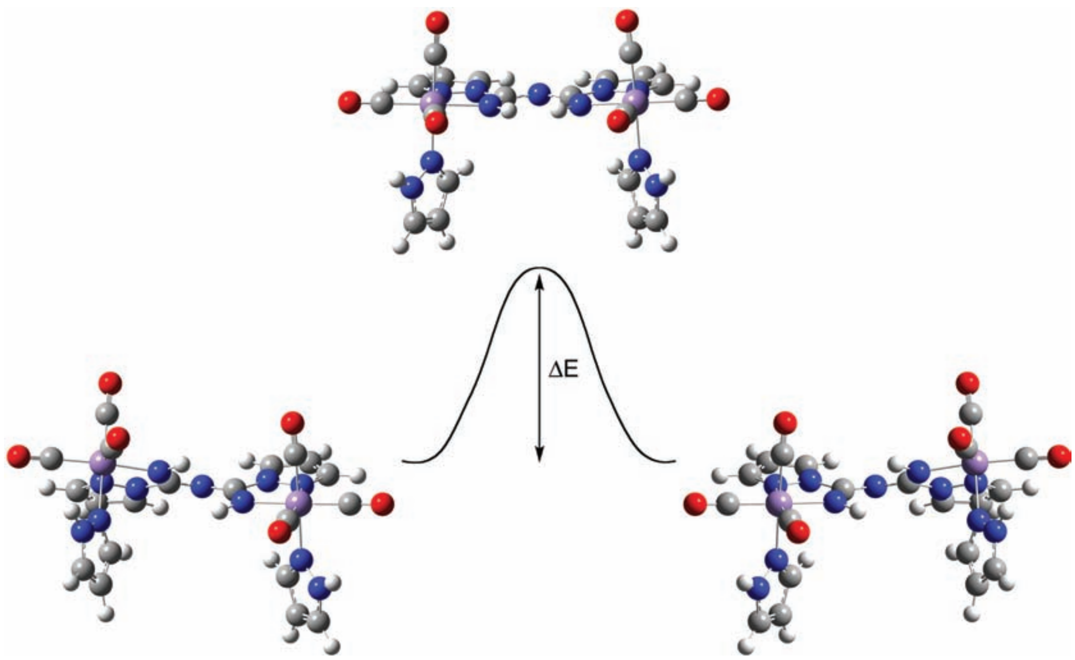

Figure 7. Energetic diagram obtained from the theoretical study on the cation of **3**.

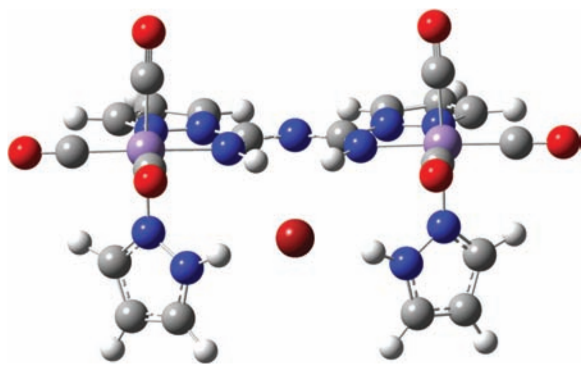

Figure 8. Planar structure obtained from the theoretical study on **3** (including the bromide anion).

The ^{1}H NMR of **3** is rather complicated because of the presence of cis and trans isomers.[13] The signals of cis isomer are immediately assigned because of their similarity with those of **4**.

The IR spectra of **3** and **4** show three bands in the C−O stretching region in solution, as expected for *fac*-tricarbonyl geometries. The frequencies are essentially the same and therefore they do not provide structural information and they are not informative.

Finally, it is interesting to note that dicyanamide does not take part in the process when using rhenium fragments, as the reactions of *fac*-[ReBr$(CO)_3(NCMe)_2$] with Na(NCNCN) and pyrazole led to the bis(pyrazole) complexes previously described,[14] probably because of the higher chemical inertness of rhenium.

CONCLUSIONS

The behavior of the sodium dicyanamide/pyrazole system clearly depends on the metallic substrate used. No pyrazolylamidino complexes are detected when *cis*-[MoCl(η^3-methallyl)$(CO)_2(NCMe)_2$] is treated with Na(NCNCN) and pzH or dmpzH, thus confirming the low tendency of this fragment to give coupling of nitriles and pyrazoles. Instead of coupling, coordination of dicyanamide and pyrazoles occurs giving dicyanamide bridging dimers containing coordinated pyrazole. Stepwise coupling with one CN bond of dicyanamide or both CN bonds occur when *fac*-[MnBr$(CO)_3(NCMe)_2$] is used as starting material, giving new pyrazolylamidino chelating ligands coordinated to one metal atom in the first case, or as bridging ligand in a binuclear complex in the second. The X-ray diffraction structure of the new compounds present some C−N bonds of the pyrazolylamidino ligands intermediate between single and double. NBO theoretical studies on these complexes allowed to deduce the electronic origin of that feature, and helped to explain the planarity of the tetradentate ligand in the bimetallic complex. The geometry of the bimetallic complex depends on the anion: both cis and trans isomers are present with bromide, whereas only the trans isomer is assembled with perchlorate.

EXPERIMENTAL SECTION

General Remarks. All manipulations were performed under N_2 atmosphere following conventional Schlenk techniques. Filtrations were carried out on dry Celite under N_2. Solvents were purified according to standard procedures.[15] [Mo(η^3-Metallyl)Cl-$(CO)_2(NCMe)_2$],[16] *fac*-[MnBr$(CO)_3(NCMe)_2$],[1a] and *fac*-[MnBr-$(CO)_3(pzH)_2$][1a] were obtained as previously described. All other reagents were obtained from the usual commercial suppliers, and used as received. ***Caution!*** *Although no difficulties were experienced with the perchlorate complex described herein, all perchlorate species should be treated as potentially explosive and handled with care.* Infrared spectra were recorded in a Perkin-Elmer RX I FT-IR apparatus using 0.2 mm CaF_2 cells for solutions or on KBr pellets for solid samples. NMR spectra were recorded in Bruker AC-300 or ARX-300 instruments in $(CD_3)_2CO$ at room temperature unless otherwise stated. NMR spectra are referred to the internal residual solvent peak for ^{1}H and $^{13}C\{^{1}H\}$ NMR. Assignment of the $^{13}C\{^{1}H\}$ NMR data was supported by DEPT experiments and relative intensities of the resonance signals. Elemental analyses were performed on a Perkin-Elmer 2400B microanalyzer

***cis*-[Mo(η^3-methallyl)$(CO)_2$(pzH)(μ-*NCNCN*-κ^2*N,N*)]$_2$ (1a).** Na-(NCNCN) (0.018 g, 0.2 mmol) and pzH (0.014 g, 0.2 mmol) were added to a solution of *cis*-[Mo(η^3-metallyl)Cl$(CO)_2(NCMe)_2$] (0.068

Table 6. ^{1}H NMR Data for 4 at Different Temperatures[a]

T	HN pzH		H^5 pzH		H^3 pzH		H^4 pzH		HNMn		H^5 pz		H^3 pz		H^4 pz	
323 K	12.34 br s	12.19 br s	7.89 br s	7.87 br s	7.62 br s	7.59 br s	6.39 br s	6.39 br s	8.10 br s	8.10 br s	8.44 br m	8.44 br m	8.67 d, J = 3	8.67 d, J = 3	6.75 t, J = 2.5	6.72 t, J = 2.5
293 K	12.49 br s	12.38 br s	7.92 d, J = 2.5	7.90 d, J = 2.5	7.62 d, J = 2	7.60 d, J = 2	6.42 br s	6.42 br s	8.24 br s	8.24 br s	8.44 d, J = 2	8.44 d, J = 2	8.71 d, J = 2.5	8.71 d, J = 2.5	6.76 t, J = 2.5	6.75 t, J = 2.5
193 K	13.11 s	13.06 s	8.09 br s	8.08 br s	7.78 br s	7.78 br s	6.49 br s	6.49 br s	8.71 br s	8.60 br s	8.58 br s	8.58 br s	8.84 d, J = 3	8.79 d, J = 3	6.87 br s	6.87 br s

[a]Coupling constants in hertz (Hz).

Scheme 6. NOEs Detected at 183 K for 4[a]

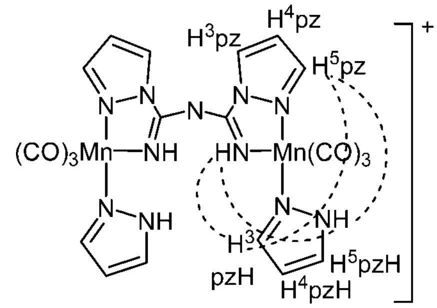

[a]For clarity, only those on one fragment of the molecule are depicted, the same NOEs are detected for the fragment on the left.

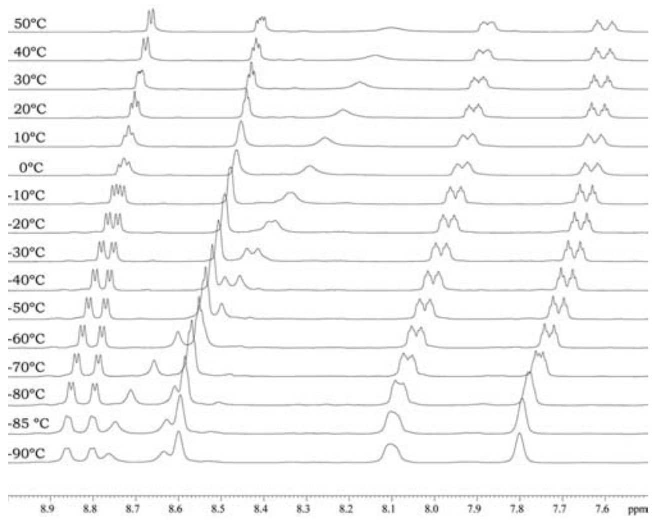

Figure 9. ^{1}H NMR spectra of **4** between 50 and −90 °C between 7.5 and 9 ppm showing H^3pz, H^5pz, HNMn, H^5pzH, H^3pzH (left to right at 50 °C).

g, 0.2 mmol) in thf (10 mL). The solution was stirred at 60 °C for 1 h, and then was filtered and concentrated in vacuo. Addition of hexane (ca. 20 mL) and cooling to −20 °C gave a yellow microcrystalline solid, which was decanted, washed with hexane (3 × 3 mL approximately), and dried in vacuo, yielding 0.028 g of **1a** (21%). Decomposition of the solid is observed even under inert atmosphere, which precluded its spectroscopic characterization and suitable C,H,N analysis. IR (thf, cm^{-1}): 2252 w, 2202 s, 1944 vs, 1861 s. IR (KBr, cm^{-1}): 3422 w, 2301 w, 2251 w, 2202 s, 1936 vs, 1850 vs, 1341 m, 1136 w, 1046 w, 771 w, 503 w. ^{1}H NMR: 0.95, 1.00, 1.16, 1.18 (s, H^{anti} methallyl), 2.13 (s, overlapped with the acetone signal, CH_3 methallyl), 3.01, 3.02, 3.10, 3.14 (s, H^{syn} methallyl), 6.35, 6.58 (s, H^4 pzH), 7.42, 7.78, 7.90, 7.97 (s, H^3 and H^5 pzH), 12.37 (br, NH), the relative intensities of the signals are variable).

***cis*-[Mo(η^3-methallyl)(CO)$_2$(dmpzH)(μ-NCNCN-κ^2N,N)]$_2$ (1b).** Na(NCNCN) (0.018 g, 0.2 mmol) and dmpzH (0.019 g, 0.2 mmol) were added to a solution of *cis*-[Mo(η^3-methallyl)Cl(CO)$_2$(NCMe)$_2$] (0.068 g, 0.2 mmol) in thf (10 mL). The solution was stirred at 60 °C for 1 h. Workup as for **1a** gave 0.033 g (22%) of **1b** as yellow crystals. Decomposition of the solid is observed even under inert atmosphere, which precluded its spectroscopic characterization and suitable C,H;N analysis. IR (thf, cm^{-1}): 2253 w, 2202 s, 1942 vs, 1860 s. IR (KBr, cm^{-1}): 3422 w, 2184 m, 2037 w, 1937 vs, 1847 s, 1325 m, 1046 w, 886 w, 670 w. ^{1}H NMR: 0.95, 1.01, 1.10, 1.14 (s, H^{anti} methallyl), 2.13 (s, overlapped with the acetone signal, CH_3 methallyl), 2.16, 2.19, 2.24, 2.28, 2.34, 2.36, 2.41, 2.46, 2.56, 2.59 (s, CH_3 dmpzH), 2.82, 3.01, 3.02, 3.05, 3.10 (s, H^{syn} methallyl), 5.89,

Table 7. Crystal Data and Refinement Details for 1b, 2a, 2b, 3, and 4

	1b	2a	2b·thf	3	4·thf
formula	$C_{34}H_{46}Mo_2N_{10}O_6$	$C_{11}H_8MnN_7O_3$	$C_{19}H_{24}MnN_7O_4$	$C_{20}H_{16}BrMn_2N_{11}O_6$	$C_{24}H_{24}ClMn_2N_{11}O_{11}$
fw	882.69	341.18	469.39	696.23	787.87
cryst system	triclinic	monoclinic	triclinic	monoclinic	orthorhombic
space group	$P\bar{1}$	$P2(1)/n$	$P\bar{1}$	$P2(1)/n$	$Pna2(1)$
a, Å	11.897(4)	7.7764(18)	8.733(7)	16.232(7)	16.046(11)
b, Å	14.105(5)	13.535(3)	10.655(8)	9.622(4)	8.880(6)
c, Å	14.454(5)	13.609(3)	13.642(11)	27.200(9)	23.199(16)
α, deg	67.379(5)	90	98.909(13)	90	90
β, deg	85.495(7)	102.601(5)	96.890(13)	97.354(7)	90
γ, deg	69.564(7)	90	107.068(13)	90	90
V, Å^3	2093.6(13)	1397.9(6)	1180.3(16)	4213(3)	3306(4)
Z	2	4	2	6	4
T, K	293(2)	298(2)	298(2)	293(2)	298(2)
d_{calc}, g cm^{-3}	1.400	1.621	1.321	1.646	1.583
$F(000)$	904	688	488	2076	1600
λ (Mo K$_\alpha$), Å	0.71073	0.71073	0.71073	0.71073	0.71073
crystal size, mm; color	0.20 × 0.06 × 0.03, yellow	0.28 × 0.16 × 0.08, yellow	0.36 × 0.25 × 0.18, yellow	0.29 × 0.28 × 0.16, yellow	0.31 × 0.24 × 0.13, yellow
μ, mm^{-1}	0.651	0.969	0.597	2.377	0.917
scan range, deg	1.53 to 23.38	2.15 to 23.29	1.53 to 28.59	1.26 to 23.29	1.76 to 24.99
absorption correction	semiempirical from equivalents	semiempirical from equivalents	semiempirical from equivalents	semiempirical from equivalents	semiempirical from equivalents
corr. factors (max, min)	1.000000, 0.363603	1.000000, 0.787786	1.000000, 0.368812	1.000000, 0.748043	1.000000, 0.714322
no of refl measured	9429	6114	11278	26351	20702
no of ref independent [R(int)]	5968 [0.0988]	2016 [0.0258]	5682 [0.0397]	6052 [0.0735]	5354 [0.1021]
no of ref observed, $I \geq 2\sigma(I)$	1912	1597	3926	4546	3066
GOF on F^2	0.840	1.000	1.161	1.113	1.192
no. of parameters	449	199	284	542	384
residuals R, wR2	0.0820, 0.2188	0.0338, 0.0878	0.0608, 0.1609	0.0760, 0.1760	0.1054, 0.2060

6.00, 6.11, 6.16 (s, H^4 pzH), 11.38 (br, NH), the relative intensities of the signals are variable).

***fac*-[Mn(pzH)(CO)$_3$(*NH*=C(pz)NCN-κ^2*N,N*)] (2a).** Na(NCNCN) (0.027 g, 0.3 mmol) and pzH (0.041 g, 0.6 mmol) were added to a solution of *fac*-[MnBr(CO)$_3$(NCMe)$_2$] (obtained from 0.083 g, 0.3 mmol of [MnBr(CO)$_5$])[1a] in thf (10 mL). The solution was stirred at 60 °C for 6 h. Workup as for **1a** gave 0.045 g (44%) of **2a** as yellow crystals. IR (thf, cm^{-1}): 2176 w, 2159 vw, 2035 vs, 1939 vs, 1927 vs. IR (KBr, cm^{-1}): 3342 s, 2188 s, 2034 vs, 1942 vs, 1924 vs, 1602 s, 1459 s, 1408 s, 1237 m, 1054 m, 772 m, 725 m, 524 m. ^{1}H NMR: 6.39 (pst, J = 2.5 Hz, H^4 pzH, 1 H), 6.66 (pst, J = 2.5 Hz, H^4 pz, 1 H), 7.65 (d, J = 1.5 Hz, H^3 pzH, 1 H), 7.89 (d, J = 2.0 Hz, H^5 pzH, 1 H), 8.22 (d, J = 2.5 Hz, H^5 pz, 1 H), 8.37 (d, J = 1.5 Hz, H^3 pz, 1 H), 12.64 (br, HN, 1 H). ^{13}C{^{1}H} NMR: 107.7 (s, C^4 pzH), 110.8 (s, C^4 pz), 131.7 (s, $C^{3,5}$ pzH), 132.9 (s, $C^{3,5}$ pz), 143.5 (s, $C^{5,3}$ pzH), 146.9 (s, $C^{5,3}$ pz), HN=C, C≡N, and CO not observed because of the low solubility of the complex. Anal. Calcd. for $C_{11}H_8MnN_7O_3$: C, 38.73; H, 2.36; N, 28.74. Found: C, 38.49; H, 2.11; N, 28.89.

***fac*-[Mn(dmpzH)(CO)$_3$(*NH*=C(dmpz)NCN-κ^2*N,N*)] (2b).** Na(NCNCN) (0.027 g, 0.3 mmol) and dmpzH (0.058 g, 0.6 mmol) were added to a solution of *fac*-[MnBr(CO)$_3$(NCMe)$_2$] (obtained from 0.083 g, 0.3 mmol of [MnBr(CO)$_5$])[1a] in thf (10 mL). The solution was stirred at 60 °C for 6 h. Workup as for **1a** gave 0.050 g (42%) of **2b** as yellow crystals. IR (thf, cm^{-1}): 2176 w, 2031 vs, 1939 vs, 1919 s. IR (KBr, cm^{-1}): 3310 m, 3143 w, 2170 s, 2030 vs, 1929 vs, 1911 s, 1613 s, 1429 s, 1283 m, 1238 w, 803 w, 650 w, 523 w. ^{1}H NMR (CD$_2$Cl$_2$): 2.12 (s, CH_3 dmpzH, 3 H), 2.28 (s, CH_3 dmpzH, 3 H), 2.54 (s, CH_3 dmpz, 3 H), 2.65 (s, CH_3 dmpz, 3 H), 5.77 (s, H^4 dmpzH, 1 H), 6.05 (s, H^4 dmpz, 1 H), 7.11 (br s, NH, 1 H), 11.88 (br s, NH, 1 H). ^{13}C{^{1}H} NMR (CD$_2$Cl$_2$): 10.9 (s, CH$_3$ dmpzH), 14.3 (s, CH$_3$ dmpz), 14.8 (s, CH$_3$ dmpzH), 15.4 (s, CH$_3$ dmpz), 106.6 (s, C^4 dmpzH), 111.8 (s, C^4 dmpz), 142.7 (s, $C^{3,5}$ dmpzH), 146.2 (s, $C^{3,5}$ dmpz), 152.6 (s, $C^{5,3}$ dmpzH), 155.5 (s, $C^{5,3}$ dmpz), HN=C, C≡N, and CO not observed because of the low solubility of the complex. Anal. Calcd. for $C_{15}H_{16}MnN_7O_3$: C, 45.35; H, 4.06; N, 24.68. Found: C, 45.53; H, 3.74; N, 24.35.

[{*fac*-Mn(pzH)(CO)$_3$}$_2$(μ-*NH*=C(pz)NC(pz)=*NH*-κ^4*N,N,N,N*)]Br (3). Compound **2a** (0.017 g, 0.05 mmol) was added to a solution of *fac*-[MnBr(CO)$_3$(pzH)$_2$] (0.018 g, 0.05 mmol) in thf (5 mL), and the solution was stirred at r.t. for 4 h. Hexane was added (ca. 10 mL), and the solution was concentrated and cooled to −20 °C, giving a yellow-orange microcrystalline solid, which was decanted, washed with hexane (3 × 3 mL approximately), and dried in vacuo, yielding 0.026 g (75%). IR (thf, cm^{-1}): 2176 w, 2035 vs, 1939 vs, 1928 s. IR (KBr, cm^{-1}): 3115 m, 2964 m, 2036 vs, 1943 vs, 1919 vs, 1615 m, 1584 s, 1435 m, 1385 m, 1261 m, 1048 w, 1027 w, 808 m, 648 m, 631 w, 561 w, 533 w, 486 w. ^{1}H NMR: 6.31 (br s, H^4 pzH, 2 H *cis*), 6.39 (br s, H^4 pzH, 2 H *trans*), 6.68 (t, J = 2 Hz, H^4 pz, 2 H *cis*), 6.73 (t, J = 2 Hz, H^4 pz, 2 H *trans*), 7.65 (br s, H^3 pzH, 2 H *cis*), 7.70 (br s, H^3 pzH, 2 H *trans*), 7.88 (br s, H^5 pzH, 2 H *cis*), 7.96 (br s, H^5 pzH, 2 H *trans*), 8.45 (d, J = 2 Hz, H^5 pz, 2 H *cis*), 8.49 (d, J = 2 Hz, H^5 pz, 2 H *trans*), 8.58 (d, J = 2 Hz, H^3 pz, 2 H *trans*), 8.64 (d, J = 2 Hz, H^3 pz, 2 H *cis*), 9.10 (br s, HNMn, 2 H *cis*, and 2 H *trans*), 13.64 (br s, HN pzH, 2 H *cis*, and 2 H *trans*). Ratio *cis*/*trans* = 1.4/1.[11] Anal. Calcd. for $C_{20}H_{16}BrMn_2N_{11}O_6$: C, 34.50; H, 2.32; N, 22.13. Found: C, 34.80; H, 2.31; N, 21.92.

[{*fac*-Mn(pzH)(CO)$_3$}$_2$(μ-*NH*=C(pz)NC(pz)=*NH*-κ^4*N,N,N,N*)]ClO$_4$ (4). AgClO$_4$ (0.011 g, 0.055 mmol) was added to a solution of **3** (0.035 g, 0.050 mmol) in thf (10 mL), and the mixture was stirred at r.t. for 4 h. Workup as for **1a** gave 0.032 g (82%) of **4**·thf. IR (thf, cm^{-1}): 2226 vw, 2176 w, 2035 vs, 1940 vs, 1927 vs IR (KBr, cm^{-1}): 3342 m, 2187 s, 2035 vs, 1930 vs, 1925 vs, 1603 s, 1459 m, 1441 m, 1407 m, 1238 w, 1054 w, 772 w, 763 w, 726 w, 689 vw, 643 w, 525 w. ^{1}H NMR: see Table 6. ^{13}C{^{1}H} NMR: 108.0 (s, C^4 Hpz), 111.0 (s, C^4 pz), 132.9 (s, $C^{3,5}$ Hpz), 133.3 (s, $C^{3,5}$ pz), 143.5 (s, $C^{5,3}$ Hpz), 147.5 (s, $C^{5,3}$pz), 158.0 (s, HNC), CO not observed. Anal. Calcd. for

$C_{24}H_{24}ClMn_2N_{11}O_{11}$ (**4**·thf): C, 36.59; H, 3.07; N, 19.56. Found: C, 36.85; H, 2.88; N, 19.31.

Computational Details. All computations were carried out using the GAUSSIAN03 package,[17] in which the hybrid method B3LYP was applied with the Becke three-parameter exchange functional,[18] and the Lee–Yang–Parr correlation functional.[19] Effective core potentials (ECP) and their associated double-ζ LANL2DZ basis set were used for the manganese and bromine atoms,[20] supplemented by an extra d-polarization function in the case of Br.[21] The light elements (O, N, C, and H) were described with the 6-31G** basis.[22] Geometry optimizations were performed under no symmetry restrictions, using initial coordinates derived from X-ray data of the same complexes, and frequency analyses were performed to ensure that a minimum structure with no imaginary frecuencies was achieved in each case. Wiberg bond indexes[23] were calculated with the NBO 5.9 program.[24]

Crystal Structure Determination for Compounds 1b, 2a, 2b, 3, and 4. Crystals were grown by slow diffusion of hexane into concentrated solutions of the complexes in thf (for **1b**, **2b**, and **4**), or CH_2Cl_2 (**2a** and **3**) at −20 °C. Relevant crystallographic details are given in Table 7. A crystal was attached to a glass fiber and transferred to a Bruker AXS SMART 1000 diffractometer with graphite monochromatized Mo K_α X-radiation and a CCD area detector. Raw frame data were integrated with the SAINT program.[25] The structure was solved by direct methods with SHELXTL.[26] A semiempirical absorption correction was applied with the program SADABS.[27] All non-hydrogen atoms were refined anisotropically. Hydrogen atoms were set in calculated positions and refined as riding atoms, with a common thermal parameter. All calculations and graphics were made with SHELXTL. Distances and angles of hydrogen bonds were calculated with PARST[28] (normalized values).[29]

■ ASSOCIATED CONTENT

Supporting Information

X-ray crystallographic data for compounds **1b**, **2a**, **2b**, **3**, (for these also experimental and simulated powder diffraction data) and **4** as a CIF. This material is available free of charge via the Internet at http://pubs.acs.org.

■ AUTHOR INFORMATION

Corresponding Author

*E-mail: fervilla@qi.uva.es. Fax: 34 983 423013. Phone: 34 983 184620.

Notes

The authors declare no competing financial interest.

■ ACKNOWLEDGMENTS

The authors thank the Spanish Ministerio de Ciencia e Innovación (CTQ2009-12111) and the Junta de Castilla y León (VA070A08 and GR Excelencia 125) for financial support. M.A. and P.G.-I. thank the MEC and the UVa respectively (FPI Programs) for their grants.

■ REFERENCES

(1) (a) Arroyo, M.; López-Sanvicente, A.; Miguel, D.; Villafañe, F. *Eur. J. Inorg. Chem.* **2005**, 4430−4437. (b) Arroyo, M.; Miguel, D.; Villafañe, F.; Nieto, S.; Pérez, J.; Riera, L. *Inorg. Chem.* **2006**, *45*, 7018−7026. (c) Antón, N.; Arroyo, M.; Gómez-Iglesias, P.; Miguel, D.; Villafañe, F. *J. Organomet. Chem.* **2008**, *693*, 3074−3080.

(2) (a) Hsieh, C.-C.; Lee, C.-J.; Horng, Y.-C. *Organometallics* **2009**, *28*, 4923−4928. (b) Khripun, A. V.; Kukushkin, V. Y.; Selivanov, S. I.; Haukka, M.; Pombeiro, A. J. L. *Inorg. Chem.* **2006**, *45*, 5073−5083. (c) Reisner, E.; Arion, V. B.; Rufinsha, A.; Chiorescu, I.; Schmid, W. E.; Keppler, B. K. *Dalton Trans.* **2005**, 2355−2364. (d) Govidaswamy, P.; Mozharivskyj, Y. A.; Kollipara, M. R. *J. Organomet. Chem.* **2004**, *689*, 3265−3274. (e) Kollipara, M. R.; Sarkhel, P.; Chakraborty, S.; Lalrempuia, R. *J. Coord. Chem.* **2003**, *56*, 1085−1091. (f) Carmona, D.; Ferrer, J.; Lahoz, F. J.; Oro, L. A.; Lamata, M. P. *Organometallics* **1996**, *15*, 5175−5178. (g) López, J.; Santos, A.; Romero, A.; Echavarren, A. M. *J. Organomet. Chem.* **1993**, *443*, 221−228. (h) Cinellu, M. A.; Stoccoro, S.; Minghetti, G.; Bandini, A. L.; Banditelli, G.; Bovio, B. *J. Organomet. Chem.* **1989**, *372*, 311−325. (i) Albers, M. O.; Francesca, S.; Crosby, A.; Liles, D. C.; Robinson, D. J.; Shaver, A.; Singleton, E. *Organometallics* **1987**, *6*, 2014−2017. (j) Gracey, G. D.; Rettig, S. T.; Storr, A.; Trotter, J. *Can. J. Chem.* **1987**, *65*, 2469−2477. (k) Romero, A.; Vegas, A.; Santos, A. *J. Organomet. Chem.* **1986**, *310*, C8−C10. (l) Jones, C. J.; McCleverty, J. A.; Rothin, A. S. *J. Chem. Soc., Dalton Trans.* **1986**, 109−111.

(3) For other examples of nucleophilic addition to metal-activated nitriles, see: (a) Pombeiro, A. J. L.; Kukushkin, V. Y. In *Comprehensive Coordination Chemistry II*; McCleverty, J. A., Meyer, T. J., Lever, A. B. P., Eds.; Elsevier: Oxford, U.K., 2004; Vol. *1*, pp 639−660. (b) Kukushkin, V. Y.; Pombeiro, A. J. L. *Chem. Rev.* **2002**, *102*, 1771−1802. (c) Michelin, R. A.; Mozzon, M.; Bertani, R. *Coord. Chem. Rev.* **1996**, *147*, 299−338.

(4) (a) Review: Hvastijová, M.; Kohout, J.; Buchler, J. W.; Boca, R.; Kozısek, J.; Jäger, L. *Coord. Chem. Rev.* **1998**, *175*, 17−45. (b) Zheng, L.-L.; Leng, J.-D.; Liu, W.-T.; Zhang, W.-X.; Lu, J.-X.; Tong, M.-L. *Eur. J. Inorg. Chem.* **2008**, 4616−4624. (c) Zheng, L.-L.; Li, H.-X.; Leng, J.-D.; Wang, J.; Tong, M.-L. *Eur. J. Inorg. Chem.* **2008**, 213−217. (d) Zheng, L.-L.; Zhang, W.-X.; Qin, L.-J.; Leng, J.-D.; Lu, J.-X.; Tong, M.-L. *Inorg. Chem.* **2007**, *46*, 9548−9557. (e) Igashira-Kamiyama, A.; Kajiwara, T.; Konno, T.; Ito, T. *Inorg. Chem.* **2006**, *45*, 6460−6466. (f) Tong, M.-L.; Wu, Y.-M.; Tong, Y.-X.; Chen, X.-M.; Chang, H.-C.; Kitagawa, S. *Eur. J. Inorg. Chem.* **2003**, 2385−2388.

(5) The molecule of **1b** is formed by two crystallographically equivalent halves because of the presence of a C_2 perpendicular to the $Mo_2(\mu\text{-}NCNCN\text{-}\kappa^2N,N)_2$ approximate plane. Table 1 collects one of the fragments. Complete tables for the whole molecule can be found in the CIF (see Supporting Information).

(6) Curtis, M. D.; Eisenstein, O. *Organometallics* **1984**, *3*, 887−895.

(7) See for example: (a) de la Pinta, N.; Martín, S.; Urtiaga, M. K.; Barandika, M. G.; Arriortua, M. I.; Lezama, L.; Madariaga, G.; Cortés, R. *Inorg. Chem.* **2010**, *49*, 10445−10454. (b) Ding, B.; Yi, L.; Wang, Y.; Cheng, P.; Liao, D.-Z.; Jiang, Z.-H.; Song, H.-B.; Wang, H.-G. *Dalton Trans.* **2006**, 665−675. (c) Batten, S. R.; Bjernemose, J.; Jensen, P.; Leita, B. A.; Murria, K. S.; Moubaraki, B.; Smith, J. P.; Toftlund, H. *Dalton Trans.* **2004**, 3370−3375. (d) Miyasaka, H.; Nakata, K.; Sugiera, K.; Yamashita, M.; Clérac, R. *Angew. Chem., Int. Ed.* **2004**, *43*, 707−711. (e) Jensen, P.; Batten, S. R.; Moubaraki, B.; Murria, K. S. *Dalton Trans* **2002**, 3712−3722. (f) Batten, R.; Jensen, P.; Moubaraki, B.; Murria, K. S. *Chem. Commun.* **2000**, 2331−2332.

(8) (a) Faller, J. W.; Haitko, D. A.; Adams, R. D.; Chodosh, D. F. *J. Am. Chem. Soc.* **1979**, *101*, 865−876. (b) Paredes, P.; Miguel, D.; Villafañe, F. *Eur. J. Inorg. Chem.* **2003**, 995−1004. (c) Arroyo, M.; García-de-Prada, M. T.; García-Martín, C.; García-Pacios, V.; García-Rodríguez, R.; Gómez-Iglesias, P.; Lorenzo, F.; Martín-Moreno, I.; Miguel, D.; Villafañe, F. *J. Organomet. Chem.* **2009**, *694*, 3190−3199. (d) Paredes, P.; López-Calzada, A.; Miguel, D.; Villafañe, F. *Dalton Trans.* **2010**, *39*, 10099−10104.

(9) See for example: (a) Reimann, R. H.; Singleton, E. *J. Chem. Soc., Dalton Trans.* **1974**, 808−813. (b) Armstrong, E. M.; Baker, P. K.; Drew, M. G. B. *Organometallics* **1988**, *7*, 319−325. (c) Fraccarollo, D.; Bertani, R.; Mozzon, M.; Belluco, U.; Michelin, R. A. *Inorg. Chim. Acta* **1992**, *201*, 15−22. (d) Thomas, S.; Young, C. G.; Tiekink, E. R. T. *Organometallics* **1998**, *17*, 182−189. (e) Hevia, E.; Pérez, J.; Riera, V.; Miguel, D.; Kassel, S.; Rheingold, A. *Inorg. Chem.* **2002**, *41*, 4673−4679.

(10) (a) Stor, G. J.; Stufkens, D. J.; Vernooijs, P.; Baerends, E. J.; Fraanje, J.; Goubitz, K. *Inorg. Chem.* **1995**, *34*, 1588−1594. (b) Schmidt, G.; Paulus, H.; van Eldik, R.; Elias, H. *Inorg. Chem.* **1988**, *27*, 3211−3214. (c) Horn, E.; Snow, M. R.; Tiekink, E. R. T. *Acta Crystallogr., Sect. C: Cryst. Struct. Commun.* **1987**, *43*, 792−794.

(11) (a) Jeffrey, G. A. *An Introduction to Hydrogen Bonding*; Oxford University Press: New York, 1997; Chapter 2. (b) Steiner, T. *Angew. Chem., Int. Ed* **2002**, *41*, 48−76.

(12) Because of the low quality of the crystal, the resulting determination is poor (high residuals). Nevertheless, the structure is included here since it confirms unambiguously the connectivity of the molecule.

(13) The presence of two isomers in solution precluded obtaining a suitable $^{13}C\{^{1}H\}$ NMR spectum of **3**.

(14) Ardizzoia, G. A.; LaMonica, G.; Maspero, A.; Moret, M.; Maschiocchi, N. *Eur. J. Inorg. Chem.* **1998**, 1503−1512.

(15) Perrin, D. D.; Armarego, W. L. F. *Purification of Laboratory Chemicals*, 3rd ed.; Pergamon Press: Oxford, U.K., 1988.

(16) Tom Dieck, H.; Friedel, H. *J. Organomet. Chem.* **1968**, *14*, 375−385.

(17) Frisch, M. J.; Trucks, G. W.; Schlegel, H. B.; Scuseria, G. E.; Robb, M. A.; Cheeseman, J. R.; Montgomery, Jr., J. A.; Vreven, T.; Kudin, K. N.; Burant, J. C.; Millam, J. M.; Iyengar, S. S.; Tomasi, J.; Barone, V.; Mennucci, B.; Cossi, M.; Scalmani, G.; Rega, N.; Petersson, G. A.; Nakatsuji, H.; Hada, M.; Ehara, M.; Toyota, K.; Fukuda, R. ; Hasegawa, J.; Ishida, M.; Nakajima, T.; Honda, Y.; Kitao, O.; Nakai, H.; Klene, M.; Li, X.; Knox, J. E.; Hratchian, H. P.; Cross, J. B.; Bakken, V.; Adamo, C.; Jaramillo, J.; Gomperts, R.; Stratmann, R. E.; Yazyev, O.; Austin, A. J.; Cammi, R.; Pomelli, C.; Ochterski, J. W.; Ayala, P. Y.; Morokuma, K.; Voth, G. A.; Salvador, P.; Dannenberg, J. J.; Zakrzewski, V. G.; Dapprich, S. A.; Daniels, D.; Strain, M. C.; Farkas, O.; Malick, D. K.; Rabuck, A. D.; Raghavachari, K.; Foresman, J. B.; Ortiz, J. V.; Cui, Q.; Baboul, A. G.; Clifford, S.; Cioslowski, J.; Stefanov, B. B.; Liu, G.; Liashenko, A.; Piskorz, P.; Komaromi, I.; Martin, R. L.; Fox, D. J.; Keith, T.; Al-Laham, M. A.; Peng, C. Y.; Nanayakkara, A.; Challacombe, M.; Gill, P. M. W.; Johnson, B.; Chen, W.; Wong, M. W.; Gonzalez, C.; Pople, J. A. *Gaussian 03*, Revision E.01; Gaussian, Inc.: Wallingford, CT, 2004.

(18) Becke, A. D. *J. Chem. Phys.* **1993**, *98*, 5648−5652.

(19) Lee, C.; Yang, W.; Parr, R. G. *Phys. Rev. B* **1988**, *37*, 785−789.

(20) Hay, P. J.; Wadt, W. R. *J. Chem. Phys.* **1985**, *82*, 299−310.

(21) Höllwarth, A.; Böhme, M.; Dapprich, S.; Ehlers, A. W.; Gobbi, A.; Jonas, V.; Köhler, K. F.; Stegman, R.; Veldkamp, A.; Frenking, G. *Chem. Phys. Lett.* **1993**, *208*, 237−240.

(22) (a) Hariharan, P. C.; Pople, J. A. *Theor. Chim. Acta* **1973**, *28*, 213−222. (b) Petersson, G. A.; Al-Laham, M. A. *J. Chem. Phys.* **1991**, *94*, 6081−6090. (c) Petersson, G. A.; Bennett, A.; Tensfeldt, T. G.; Al-Laham, M. A.; Shirley, W. A.; Mantzaris, J. *J. Chem. Phys.* **1988**, *89*, 2193−2218.

(23) Wiberg, K. *Tetrahedron* **1968**, *24*, 1083−1096.

(24) Glendening, E. D.; Badenhoop, J. K.; Reed, A. E.; Carpenter, J. E.; Bohmann, J. A.; Morales, C. M.; Weinhold, F. *NBO*, 5.9; Theoretical Chemistry Institute, University of Wisconsin: Madison, WI, 2009; http://www.chem.wisc.edu/~nbo5.

(25) *SAINT+, SAX area detector integration program*, Version 6.02; Bruker AXS, Inc.: Madison, WI, 1999.

(26) (a) Sheldrick, G. M. *SHELXTL, An integrated system for solving, refining, and displaying crystal structures from diffraction data*, Version 5.1; Bruker AXS, Inc.: Madison, WI, 1998. (b) Sheldrick, G. M. *Acta Crystallogr.* **2008**, *A64*, 112−122.

(27) Sheldrick, G. M. *SADABS, Empirical Absorption Correction Program*; University of Göttingen: Göttingen, Germany, 1997.

(28) (a) Nardelli, M. *Comput. Chem.* **1983**, *7*, 95−98. (b) Nardelli, M. *J. Appl. Crystallogr.* **1995**, *28*, 659.

(29) (a) Jeffrey, G. A.; Lewis, L. *Carbohydr. Res.* **1978**, *60*, 179−182. (b) Taylor, R.; Kennard, O. *Acta Crystallogr.* **1983**, *B39*, 133−138.